

ULTRA-SHORT ELECTRON BUNCH AND X-RAY TEMPORAL DIAGNOSTICS WITH AN X-BAND TRANSVERSE DEFLECTOR

Y. Ding, P. Emma, J. Frisch, Z. Huang, H. Loos, P. Krejcik,
M-H. Wang (SLAC, Menlo Park, California)
C. Behrens (DESY, Hamburg, Germany)

Abstract

The measurement of ultra-short electron bunches on the femtosecond time scale constitutes a very challenging problem. In X-ray free-electron laser facilities such as the Linac Coherent Light Source (LCLS), generation of sub-ten femtosecond X-ray pulses is possible, and some efforts have been put into both ultra-short electron and X-ray beam diagnostics. Here we propose a single-shot method using a transverse rf deflector (X-band) after the undulator to reconstruct both the electron bunch and X-ray temporal profiles. Simulation studies show that about 1 fs (rms) time resolution may be achievable in the LCLS and is applicable to a wide range of FEL wavelengths and pulse lengths. The jitter, resolution and other related issues will be discussed.

INTRODUCTION

The successful operation of the Linac Coherent Light Source (LCLS) [1], with its capability of generating free-electron laser (FEL) X-ray pulses from a few femtoseconds (fs) up to a few hundred fs, opens up vast opportunities for studying atoms and molecules on this unprecedented ultra-short time scale. However, tremendous challenges remain in the measurement and control of these ultrashort pulses with femtosecond precision, for both the electron beam (e-beam) and the X-ray pulses.

For ultrashort e-beam bunch length measurements, a standard method has been established at LCLS using an S-band radio-frequency (rf) deflector, which works like a streak camera for electrons and is capable of resolving bunch lengths as short as ~ 10 fs rms [1]. However, the e-beam with low charges of 20 pC at LCLS, which is expected to be less than 10 fs in duration, is too short to be measured using this transverse deflector [2].

The measurement of the electron bunch length is helpful in estimating the FEL X-ray pulse duration. However, for a realistic beam, such as that with a Gaussian shape or even a spiky profile, the FEL amplification varies along the bunch due to peak current or emittance variation. This will cause differences between the temporal shape or duration of the electron bunch and the X-ray pulse. Initial experiments at LCLS have revealed that characterization of the X-ray pulse duration on a shot-by-shot basis is critical for the interpretation of the data. However, a reliable x-ray pulse temporal diagnostic tool is not available so far at the LCLS.

We propose a novel method in this paper to characterize the FEL X-ray pulse duration and shape. A transverse

rf deflector is used in conjunction with an e-beam energy spectrometer, located after the FEL undulator. By measuring the difference in the e-beam longitudinal phase space between FEL-on and FEL-off, we can obtain the time-resolved energy loss and energy spread induced from the FEL radiation, allowing the FEL X-ray temporal shape to be reconstructed.

RF DEFLECTOR AND SYSTEM LAYOUT

The idea of using an rf deflecting structure to kick the electron beam was first proposed in 1960s [3], and has been recently used for e-beam bunch length measurements in FELs and other accelerator facilities [4]. We assume the bunch is deflected in horizontal plane by the high-frequency time-variation of the deflecting fields, where the resulting horizontal beam width measured on a downstream screen represents a single-shot measure of the absolute bunch length. This horizontally “streaked” e-beam is then sent to an energy spectrometer, which is composed of dipoles and quadrupoles providing large vertical momentum dispersion. With this setup the e-beam longitudinal phase space (time and energy) is mapped into the transverse dimensions (horizontal and vertical).

In the FEL process, the interaction between an e-beam and an electromagnetic wave leads to e-beam energy modulation at the fundamental radiation wavelength. As electrons wiggle in the undulator, a periodic density modulation (the so-called “microbunching”) at the radiation wavelength builds up. The microbunched e-beam then emits coherent radiation at the expense of the electron kinetic energy. The collective interaction of the beam-radiation system leads to an exponential growth of the radiation intensity along the undulator distance. As a result, it causes electron energy loss and energy spread increase and FEL power reaches saturation. At LCLS, the typical FEL-induced electron energy loss at saturation is more than 10 MeV [1]. To obtain the X-ray temporal profile, we first suppress the FEL process (e.g. by kicking e-beam to make a local oscillating orbit inside the undulator) and measure the e-beam time-energy phase space, from which we can get the e-beam temporal profile and also achieve a baseline on the energy loss. Next, the FEL is restored and measure the time-energy phase space again for each bunch. By subtracting the baseline image measured with FEL-off, we can obtain the time-resolved energy loss or energy spread due to FEL radiation, shot by shot. The X-ray temporal power profile is then determined by combining the e-beam current profile and the time-resolved energy loss.

Figure 1 shows the beamline layout of the diagnostic system to be installed at the end of the LCLS main undulator.

APPLICATION OF THE METHOD

The working principle of transverse rf deflectors for time-resolved beam diagnostics is described in many references, e.g. in [4]. The deflecting force imparts a transverse momentum on the bunch and the resulting kick angle is transported through a transfer matrix with angular-to-spatial element $R_{12} = (\beta_{xd}\beta_{xs})^{1/2}\sin\Delta\Psi$. Here β_{xd} and β_{xs} are the horizontal beta functions at the deflector and the screen, respectively, and $\Delta\Psi$ is the horizontal beta-tran phase advance from deflector to screen. The transverse position of each ultra-relativistic electron on the screen is then given

$$\Delta x(t) = \frac{eV_0}{pc} \sqrt{\beta_{xd}\beta_{xs}} |\sin\Delta\Psi| \left(\frac{2\pi}{\lambda} c t \cos\varphi + \sin\varphi \right). \quad (1)$$

From Eq. (1) it is clear that for bunch length measurement, operating at the zero-crossing phase ($\varphi = 0$) gives the best streaking effects with the horizontal beam size corresponding to bunch length ($\sigma_x \propto c\sigma_t$), while $\sin\varphi \neq 0$ gives a centroid offset which can be used for calibration ($\langle\Delta x\rangle \propto \sin\varphi$). For example, by measuring the horizontal centroid offset with a small rf phase shift around zero-crossing, the size of horizontal dimension is calibrated relative to the absolute RF wavelength. From Eq. (1), near zero-crossing, the time calibration factor can be written as

$$S = \frac{\sigma_x}{c\sigma_t} = \frac{eV_0}{pc} \sqrt{\beta_{xd}\beta_{xs}} |\sin\Delta\Psi| \frac{2\pi}{\lambda}. \quad (2)$$

For the LCLS e-beam high-energy case of 14 GeV, based on the parameters listed in Table 1, $S = 128$. This means if the measured horizontal beam size $\sigma_x = 128\mu\text{m}$, the actual bunch length is $c\sigma_t = 1\mu\text{m}$. Note that an X-band rf deflector has been chosen over S-band like the original transverse deflector [3] in order to impart a stronger sweep to the beam and improve the temporal resolution.

The vertical beam size measured after the vertically-bent spectrometer represents the electron energy deviation, which is given by

$$\Delta y = \eta_y \delta, \quad (3)$$

where η_y is the vertical momentum dispersion function at the screen, and δ is the relative energy deviation before the energy spectrometer. Note now we have a two-dimensional image with x representing to time, and y representing to energy.

Temporal resolution $\sigma_{t,r}$ and energy resolution $\sigma_{E,r}$ can be defined as

$$\sigma_{t,r} = \frac{\sigma_{x0}}{cS}, \quad \sigma_{E,r} = \frac{\sigma_{y0}}{\eta_y} E_0, \quad (4)$$

where σ_{x0} or σ_{y0} is the nominal transverse beam size at the screen (i.e., in the absence of deflecting voltage for σ_{x0} ,

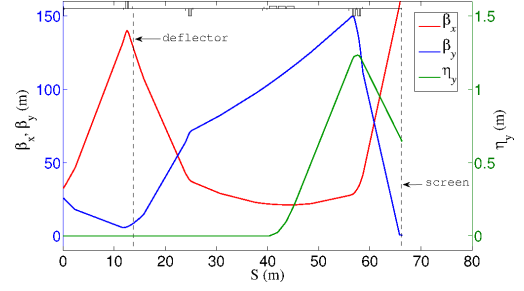


Figure 2: The optics layout for this diagnostics. The locations of the deflector and screen are marked in the picture.

and in the absence of dispersion for σ_{y0}), and E_0 is the average electron energy.

As seen from Eq. (1) and (3), the beam transportation optics should be optimized to achieve the best resolution. Larger horizontal beta function at deflector and smaller vertical beta function at screen are preferred. The optics beta and dispersion functions for the high-energy (14 GeV) case are shown in Fig. 2 for the existing LCLS beamline magnets after their strengths have been adjusted to optimize the beta functions. A very similar optics setup has also been achieved at low electron-energy (4.3 GeV) for soft X-ray generation.s

The main parameters are summarized in Table 1, based on a normalized projected-emittance of $0.6\mu\text{m}$. The potential temporal resolution is ~ 1 fs rms for LCLS soft X-rays, and ~ 2 fs for hard X-rays.

Table 1: X-band transverse deflector parameters [5].

Parameter	Symbol	Value	Unit
RF frequency	f	11.424	GHz
Deflecting structure length	L	2×1	m
RF input power	P	40	MW
Deflecting voltage (on crest)	V_0	48	MV
Soft X-ray (e-beam 4.3 GeV)			
Calibration factor	S	400	
Temporal resolution (rms)	$\sigma_{t,r}$	~ 1	fs
Energy resolution (rms)	$\sigma_{E,r}$	56	keV
Hard X-ray (e-beam 14 GeV)			
Calibration factor	S	128	
Temporal resolution (rms)	$\sigma_{t,r}$	~ 2	fs
Energy resolution (rms)	$\sigma_{E,r}$	100	keV

SIMULATION STUDIES

Start-to-end simulations have been carried out to verify this scheme. IMPACT-T [6] and ELEGANT [7] codes have been used in the injector and main linac, including bunch compressors. In the undulator, a 3-dimensional (3D) FEL simulation code GENESIS [8] has been adopted for FEL simulations, where the resistive wake fields from undulator chamber and the spontaneous undulator radiation are

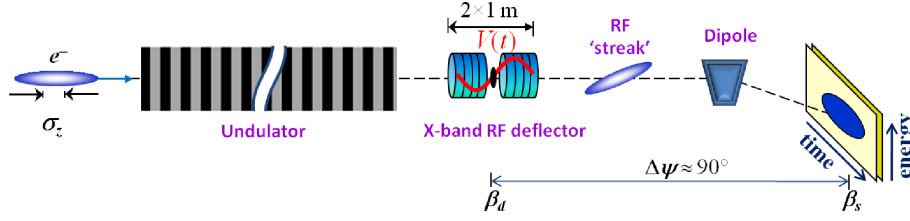


Figure 1: A layout of the diagnostic system with a transverse rf deflector and an energy spectrometer.

also included. At the end of the undulator, the dumped particles are used again by ELEGANT to track them through the transverse deflector and energy spectrometer down to the dump screen. From the simulated images at the dump screen, we can analyze the X-ray pulse duration.

We first show an example of the LCLS hard X-ray case (radiation wavelength of 1.5 Å, e-beam energy of 13.6 GeV, total undulator length of 132m including breaks) with a nominal operating charge of 250 pC. The average e-beam peak current is about 3 kA. Since the resistive wake fields in the linac rf structure introduce a third-order nonlinear curvature in the longitudinal phase space, we typically have a “double-horn” shape in the current profile. It is of great importance and interest to characterize the lasing process from this complicated bunch shape.

Figure 3(a) and 3(b) shows the simulated “measurements” of the projected transverse images at the dump screen, with the horizontal axis representing time, and the vertical axis representing energy. Clearly, we can see the difference in the energy dimension between FEL-on and FEL-off. From the case of FEL-off (Fig. 3(a)), we get the time-resolved e-beam energy and energy spread. The major collective effects include those from undulator chamber wakes, undulator spontaneous radiation, transverse deflecting effect and coherent synchrotron radiation (CSR) in spectrometer dipoles. When switched on, the FEL radiation introduces an additional energy loss ($\Delta E_{FEL}(t)$) and energy spread. From the two measurements we can subtract the baseline image in the FEL-off mode and determine the time-sliced energy loss or energy spread increase purely induced from FEL radiation:

The horizontal projection of the images in Fig. 3(a) and 3(b) represents the e-beam temporal profile. The transverse deflector method provides an additional technique for eliminating systematic correlation errors. The upstream bunch compressors in the LCLS are in the horizontal plane and the CSR from their bends introduces a transverse kick to the electrons which is correlated to their longitudinal position in the bunch [9]. This correlation between the horizontal and longitudinal planes can affect the phase space reconstruction technique because the deflector also streaks the beam horizontally. This effect can be canceled by performing a second measurement at the other rf zero-crossing phase, 180° from the first measurement [10]. Figure 3(c) shows the reconstructed e-beam current profile ($I(t)$) from two zero-crossing phases comparing the original one.

With the obtained time-sliced energy loss and current,

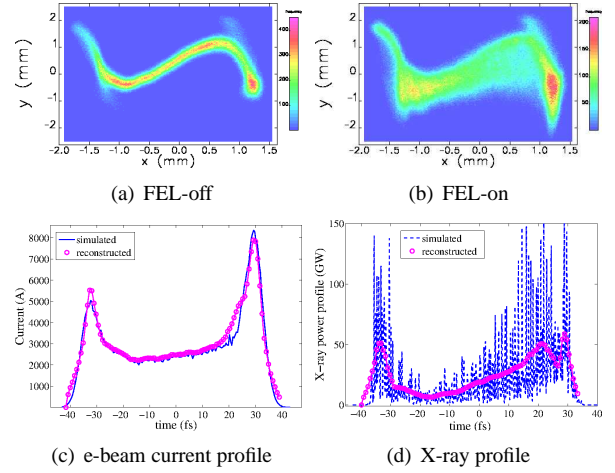


Figure 3: The simulated images on the screen representing e-beam longitudinal phase space for FEL-off (a) and FEL-on (b). The bunch charge is 250 pC with an energy of 13.6 GeV. (c) and (d) show the reconstructed e-beam current and FEL X-ray profiles comparing with the simulated ones. Bunch head is to the left.

the X-ray power profile is directly determined with an absolute power scale ($P(t) = \Delta E_{FEL}(t) \times I(t)$). The reconstructed X-ray profile from the energy loss for this hard X-ray example is shown in Fig. 3(d). Since LCLS is operating in the self-amplified spontaneous emission (SASE) mode, there are many longitudinal spikes whose typical width is ~ 0.2 fs in this hard X-ray wavelength. The reconstructed pulse shape is a smooth approximation to the actual profile, where the finer spikes are smeared out by the limited temporal resolution. Using the energy spread data we get a similar X-ray profile. To obtain the absolute power scale from the energy spread analysis requires an additional measurement of the total X-ray pulse energy.

Comparing the e-beam current profile and the X-ray profile shown in Fig. 3, we can see that the shape of the X-ray profile deviates from the e-beam current profile, with less lasing right after the horn at the head of the bunch. This is the result of wakefields in the undulator chamber from the horn at the head of the bunch suppressing the FEL lasing.

Low charge operation mode with 20 pC at LCLS has been used in many X-ray user experiments to produce X-ray pulses of a few fs duration [2]. Since these short X-ray pulses typically only have a few spikes, there is a large variation on the pulse shape. This makes the measurement of the actual X-ray pulse profile even more critical. We show

an example of the soft X-ray case right after saturation. The bunch charge is 20 pC and energy is at 4.3 GeV. In the second bunch compressor the e-beam is over-compressed so we can have a Gaussian-like current profile to generate a shorter X-ray pulse [2]. The longitudinal phase space simulated at the dump screen is shown in Fig. 4. Compare the two images with FEL-off and FEL-on, we obtained the X-ray profile (Fig. 4(d)). The e-beam is about 4 fs FWHM, and the FEL profile in this snapshot has one main spike, and two small side spikes. Comparing the reconstructed profiles with the simulated ones, we see some distortions in the profile peaks but still it is very encouraging. Running into the deep saturation regime, the slippage effect between FEL and e-beam may affect the shape of the reconstructed X-ray power profile, especially for long-wavelength radiations. In the X-ray wavelengths, this slippage effect after saturation is not a problem.

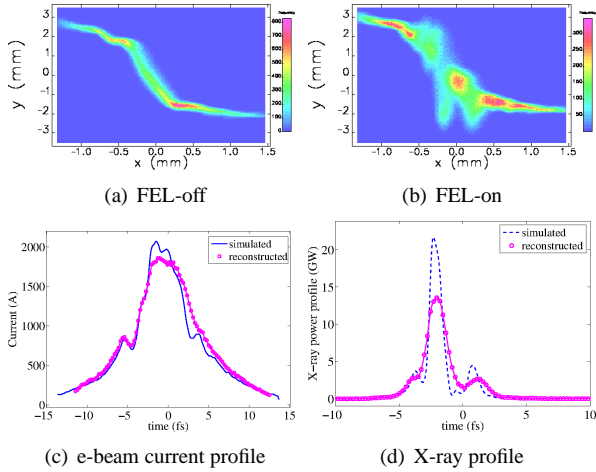


Figure 4: The simulated images on the screen representing e-beam longitudinal phase space for FEL-off (a) and FEL-on (b). The bunch charge is 20 pC with an energy of 4.3 GeV. (c) and (d) show the reconstructed e-beam current and FEL X-ray profiles comparing with the simulated ones. Bunch head is to the left.

DISCUSSIONS AND SUMMARY

As described earlier, we suppress FEL lasing process and record the e-beam longitudinal phase space as a baseline, then compare the FEL-on case with the saved baseline image to analyze the FEL X-ray profile. The pulse-by-pulse jitter issues have to be considered during the measurements. By choosing the X-band rf deflector, an increased temporal resolution has been achieved, but the price to be paid is an increased sensitivity to phase jitter between the bunch arrival time and the X-band rf system. This must be minimized by designing tight rf phase tolerances into the system. The present achievable X-band rf phase stability could be $< 0.1^\circ$, however, the measured LCLS arrival time jitter is ~ 50 fs rms [1]. This beam arrival time jitter makes the calibration very difficult. At LCLS, two phase cavities located after the undulator are used to measure the beam

arrival time with an accuracy of ~ 10 fs rms [11]. These arrival time data measured from the phase cavities can be used to correct the timing jitter during the transverse deflector calibration measurements. With this correction we can achieve a pretty good calibration within a reasonable rf phase range based on multishots average. Since we operate at the zero-crossing phase region which is quite linear, these rf phase jitter and beam arrival jitter does not affect the phase space measurement, though a relatively large screen should be considered for the system design. The e-beam pulse-by-pulse energy jitter can also be corrected with the beam position monitors (BPMs) in the dogleg before the undulator. The transverse jitter out of the undulator is small and does not cause additional effect on the measurement.

In summary, we have shown that the proposed transverse rf deflector located after the FEL undulator has the potential to reconstruct the X-ray temporal profiles by measuring the e-beam longitudinal phase space with a very high resolution down to a few fs. This single-shot method is widely applicable to any radiation wavelength, SASE or seeded FEL mode, without interruption to user operation. This data can be delivered to the X-ray experiments in real time on a pulse by pulse basis. In addition, the e-beam bunch length is also obtained, proving a useful tool for a detailed study on the FEL lasing process.

The X-band transverse deflecting structure for LCLS has been designed, and one of them is ready to use [5]. The most expensive parts are rf modulator and klystron. Together with other subsystems such as the LLRF, mechanical and vacuum, waveguide system and machine protection system, it will take about 2 years to get this diagnostic tool ready at LCLS in 2013.

ACKNOWLEDGEMENTS

We thank G. Bowden, V. Dolgashev, J. Wang, J. Welch and D. Xiang for helpful discussions. This work was supported by Department of Energy Contract No. DE-AC02-76SF00515.

REFERENCES

- [1] P. Emma *et al.*, Nat. Photon. **4**, 641 (2010).
- [2] Y. Ding *et al.*, Phys. Rev. Lett. **102**, 254801 (2009).
- [3] G. Loew, O. Altenmueller, SLAC-PUB-135, 1965.
- [4] For example, see R. Akre *et al.*, EPAC 2002, p1882; M. Röhrs *et al.*, PRST-AB **12**, 050704 (2009)
- [5] J. Wang and S. Tantawi, LINAC 08, Victoria, BC, Canada.
- [6] J. Qiang *et al.*, PRST-AB **9**, 044204 (2006).
- [7] M. Borland, Advanced Photon Source LS-287, 2000.
- [8] S. Reiche *et al.*, NIM A **429**, 243 (1999).
- [9] K. Bane *et al.*, PRST-AB **12**, 030704 (2009).
- [10] H. Loos *et al.*, FEL2005, p632, Stanford, CA (2005).
- [11] A. Brachmann *et al.*, IPAC10; see also SLAC-PUB-14234.